

## **TRIBOINFORMATICS: MACHINE LEARNING METHODS FOR FRICTIONAL INSTABILITIES**

**Michael Nosonovsky<sup>1,2</sup>, Aleksandr S. Aglikov<sup>2</sup>**

<sup>1</sup>University of Wisconsin-Milwaukee, Mechanical Engineering Department, USA

<sup>2</sup>ITMO University, Infochemistry Scientific Center, Russia

**Abstract.** *The study of friction is traditionally a data-driven area with many experimental data and phenomenological models governing structure-property relationships. Triboinformatics is a new area combining Tribology with Machine Learning (ML) and Artificial Intelligence (AI) methods, which can help to establish correlations in data on friction and wear. This is particularly relevant to unstable motion, where deterministic models are difficult to build. There are several types of friction-induced instabilities including those caused by the velocity dependency of dry friction, coupling of friction with another process (wear, heat generation, etc.), the elastic Adams instabilities, and others. The onset of sliding is also an unstable process. ML/AI methods, such as Topological Data Analysis and various ML algorithms, which have been already used for various aspects of data analysis on friction, can be applied also to the frictional instabilities.*

**Key words:** *Frictional instabilities, Painlevé paradoxes, Triboinformatics, Machine learning*

### 1. INTRODUCTION

Due to the extremely interdisciplinary and multiscale character of tribological processes, new mathematical and computational methods rapidly evolve [1]. Many current problems of contact mechanics and tribology are complex dynamic problems, which often lead to instabilities and require new mathematical methods, models, and algorithms. Thus, Ostermeyer and co-workers proposed a boundary layer machine approach for the modeling of wear [2]. Popov and co-workers applied several new methods including non-linear Diffusion-Reaction models of cellular processes [3], the Burrige-Knopoff model combined with Voronoi tessellations to study the stick-slip instability for the state-and-rate

---

Received: December 08, 2023 / Accepted March 09, 2024

**Corresponding author:** Michael Nosonovsky  
University of Wisconsin-Milwaukee, 3200 N Cramer St., Milwaukee WI 53217 USA  
ITMO University, 9 Lomonosova St., St. Petersburg, Russia  
E-mail: nosonovs@uwm.edu

friction [4], the effects of dynamic menisci on adhesion [5], a method to solve viscoelastic contact problems with arbitrary loading histories [6], and an energetic criterion for adhesion in viscoelastic contacts with non-entropic surface interactions [7]. Forsbach and co-authors [8] investigated a two-scale FEM-BAM approach for fingerpad friction under electroadhesion. Many of new multi-scale and dynamic applications are related to biomimetic and biocompatible applications [3, 9-10]. Various Machine Learning (ML) algorithms have been used successfully for similar engineering problems including the k-Nearest Neighbor (kNN), Decision Trees (DT), and Random Forests (RF) [11, 12].

Stability analysis has been the subject of intensive studies in Mechanics and the theory of Dynamical Systems since at least the middle of the 19<sup>th</sup> century. The Theory of Stability addresses the stability of equilibria states and stability of solutions of differential equations of dynamical systems, under small perturbations of initial conditions [13]. Typically, a dynamical system is represented by a point in that system's configuration space  $(x_1, x_2, \dots, x_n)$ , where  $x_i$  are coordinates and  $n$  is the total number of degrees of freedom, and by a governing differential equation which establishes the evolution of the system in the time domain.

Different approaches to the stability analysis have been developed to provide stability criteria: Lyapunov stability, algebraic stability (the Routh–Hurwitz stability criterion), frequency stability analysis (the Nyquist stability criterion), Poincare diagrams, structural stability, etc. [13]

Traditionally physicists and engineers are trying to ensure that their systems are stable and concentrate on stable behavior. However, the analysis of the behavior of unstable systems is much more difficult. The stable motion is deterministic and predictable since the state of the system at any instance of time is defined by the initial conditions. Contrary to that, unstable motion is virtually unpredictable since any small fluctuation or error tends to grow exponentially, and after a short time, it becomes impossible to predict the position of a system in the configurational space. Thus, turbulence remains a very difficult problem to handle [14]. For the analysis of unstable behavior, statistical methods can be used, and novel Machine Learning (ML) and data science algorithms can be applied [15]. The application of ML methods in tribology is a new area of research referred to as Triboinformatics [16].

There are different types of instabilities in fluid mechanics including the Rayleigh–Taylor instability, Plateau–Rayleigh instability, Rayleigh–Bénard instability, Kelvin–Helmholtz instability, Saffman–Taylor instability and many others. No comprehensive classification of fluid instabilities has been suggested so far. While fluid mechanics involves many types of instability, solid mechanics also can lead to unstable motion. In particular, dry friction can lead to the so-called frictional instabilities [17].

Dry friction is governed by the Coulomb friction law,  $F = \mu W$ , which relates the friction force,  $F$ , to the normal load force,  $W$ , through the coefficient of friction (COF),  $\mu$  [18]. Friction is usually thought of as a stabilizing factor, however, can lead to destabilization under several circumstances. This includes the situations when the COF depends upon the sliding velocity (the so-called “frictional weakening” when COF decreases with increasing velocity) or upon other parameters, such as the temperature at the frictional interface, or when friction is combined with the constitutive law of the material, such as the linear elastic dependency between stresses and strains of the material [17].

There are two types of dry friction: the static and kinetic friction, which correspond to the stick and slip states or to the states of rest and motion of the dynamical systems (Table

1). Typically, the static friction force is greater than the kinetic friction, which can be viewed as another manifestation of the frictional weakening, and it can lead to the so-called stick-slip self-excited vibrations. In terms of rheological properties of materials, friction corresponds to the plasticity. The transition to the plastic flow is sometimes viewed as a phase transition [19].

There are situations when it is useful to introduce the third state which is in a sense in between the static and kinetic friction. This is the ultraslow motion, when the rate of deformation is comparable with relaxation rates of the involved materials. The unstable motion can also be viewed as the third state, in addition to the states of rest and of deterministic stable motion. Some solutions, which result in instabilities, may originate due to ill-posedness of the dynamic problem. Nosonovsky and Breki [20] suggested that a three-valued logic can be applied to such cases. Three-valued logic is an algebraic approach in which a logical variable,  $P$ , can have a third value  $P = \text{undefined}$ , in addition to  $P = \text{true}$  and  $P = \text{false}$  of the Boolean logic (Table 1). Moreover, it is suggested that ML approaches can be applied to the unstable motion to establish correlations in data, because traditional deterministic methods fail to predict the state of the system due to exponentially growing fluctuations. In the present paper we will review main types of frictional instabilities and will expand the ternary logic approach for the frictional instabilities.

**Table 1** Instability and the non-binary character of motion and friction

	Initial State	Opposite State	Third State
Motion	Rest	Motion	Unstable Motion
Friction	Stick	Slip	Ultraslow Motion
Material	Elastic	Plastic	Relaxation / Creep
Logical Predicate, $P(x)$	$P(x)=\text{True}$	$P(x)=\text{False}$	$P(x)=\text{Undefined}$
Modeling approach	Statics	Dynamics	Machine Learning

## 2. FRICTION-INDUCED VIBRATIONS AND INSTABILITIES

In this section we will discuss different types of frictional instabilities. Since some of these instabilities are related to the ill-posedness of the dynamic problems with dry friction, we will start from the discussion of the frictional paradoxes.

### 2.1 Painlevé Paradoxes

We start the discussion of friction-induced instabilities with the Painlevé paradoxes, which are not instabilities *per se*; however, they are related to some frictional instabilities and may provide an interesting perspective to understand the latter [20-24].

Painlevé paradoxes can be found in simple (1DOF) mechanical systems with dry friction consisting of rigid undeformable bodies (sliders and connecting rods)

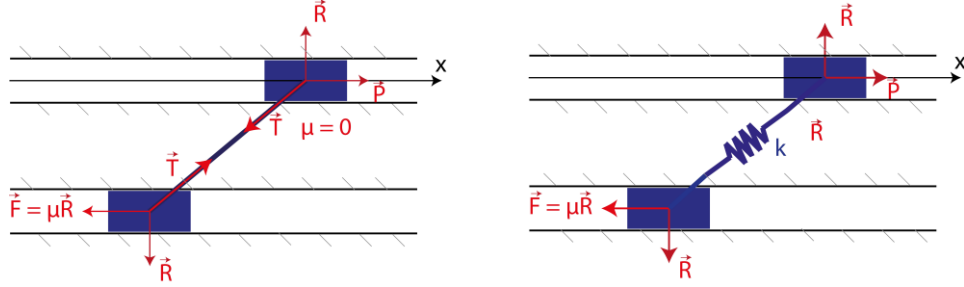


**Fig. 1** (a) The setup for the Painlevé paradox (two sliders connected by a coupler) and (b) introduction of an elastically compliant link with the spring coefficient  $k$

A simple example of the Painlevé paradox is found in the system consisting of two sliders connected by a rigid coupler link of length  $l$  (under angle  $\varphi$ ) and sliding in parallel grooves (Fig. 1a). Both sliders have the same mass  $m$ ; however, friction in the upper groove is negligible ( $\mu=0$ ), while the lower slider is subject to finite friction with the COF  $\mu=0$ . An external force  $P$  is applied to the upper slider parallel to the groove. The normal reaction force  $R$  acts at the upper slider, so that the tension force in the link is  $T = R/\sin(\varphi)$ , and the friction force is  $F = \mu|R|\text{sign}(V)$ ; the direction of the friction force depends on the sign of the sliding velocity  $V = \dot{x}$ .

The equations of motion of the system are given by

$$2m\ddot{x} = P - \mu|R|\text{sign}(\dot{x}) \quad (1)$$

$$m\ddot{x} = P - R/\tan\varphi \quad (2)$$

When COF is small so that for  $\mu \tan(\varphi) < 2$  assuming motion in the positive direction ( $V > 0, P > 0$ ), the equations of motion have a solution

$$m\ddot{x} = P \frac{1 - \mu \tan\varphi}{2 - \mu \tan\varphi} \quad (3)$$

and assuming motion in the negative direction ( $V < 0, P < 0$ ),

$$m\ddot{x} = P \frac{1 + \mu \tan\varphi}{2 + \mu \tan\varphi} \quad (4)$$

However, if  $V < 0$  and  $\mu \tan(\varphi) > 2$ , an additional solution exists

$$m\ddot{x} = P \frac{1 - \mu \tan\varphi}{2 - \mu \tan\varphi} \quad (5)$$

In case of  $V > 0$  and  $\mu \tan(\varphi) < 2$ , no solution exists at all [20].

The Coulomb-Amontons' law of dry friction is not always logically compatible with the laws of Newtonian mechanics. This is why the paradoxes, i.e., the situations when the solution is not unique or non-existent, arise in some case. In mathematics, the logically inconsistent problem is called *ill-posed*, and various ways of regularizing such problems exist. One possibility is the use of the inconsistent logic, such as the ternary (three-valued) logic.

Nosonovsky and Breki [20] suggested regularizing the paradox by using the ternary logic with the logical variable  $P_i \equiv (\dot{x}_i = 0)$  characterizing the state of the system as "rest"

( $P_i = true$ ), “motion” ( $P_i = false$ ), and “paradox” ( $P_i = undefined$ ). The undefined state is a paradoxical situation when no solution or non-unique solutions exist.

The standard logical operations of the three-valued logic can be defined, thus, if at least one part of the dynamical system is in the paradox state, the entire system is in the paradox state, and so on. The overall state of the system is given by the conjunction of the degrees of freedom  $P = P_1 \wedge P_2 \wedge \dots \wedge P_n$ . Thus, the system is at rest if all velocities are defined and equal to zero, the system is moving if at least one velocity is defined and non-zero, and the system is undefined otherwise. Similarly, the stability can be defined with the logical variable  $S_i \equiv P_i \vee \bar{P}_i$ , so that the entire system is stable when and only when all its parts are stable,  $S = S_1 \wedge S_2 \wedge \dots \wedge S_n$ .

If the link is compliant (elastically deformable), the paradox is resolved [21-22]; however, friction-induced instabilities can originate in a compliant system (Fig. 1b). In the next section we will discuss the ill-posedness of the problems with frictional instabilities.

## 2.2 Frictional Elastic Instabilities

In the previous section, we established the relation of the frictional paradoxes to frictional instabilities. The most common case of frictional elastic instabilities are the so-called Adams instabilities, which arise during frictional sliding of two elastic half-spaces with different elastic properties (i.e., with the elastic moduli  $E_1$  and  $E_2$ , densities  $\rho_1$  and  $\rho_2$ , and Poisson’s ratios  $\nu_1$  and  $\nu_2$ ) pressed together by a normal force per area,  $W$ , applied at infinity (Fig. 2a). The contact is modeled in the 2D plain-strain elasticity. The sliding is driven by a constant external shear force per area,  $P$ , applied at the infinity, so that the system is not conservative (work is done against friction).

During the frictionless contact of two elastic half-spaces, the interfacial waves, also referred to as Slip Waves or Generalized Rayleigh Waves (GRW), can propagate along the interface. The GRW is a generalization of the elastic surface wave (Rayleigh Wave) propagating along the surface of a single elastic half-space. The amplitude of the surface wave decreases exponentially with the distance from the surface. Similarly, the amplitude of the GRW decreases with the distance from the interface in both half-spaces.

Depending on the elastic properties of the sliding bodies and the COF, a self-excited dynamic instability can rise, in the form of destabilized interfacial elastic waves (GRW) whose amplitude grows exponentially with time [25]. Frictional elastic instabilities emerge also during sliding of a periodic wavy elastic surface against a flat elastic half-space [26]. The degree of instability (the rate of growth of the wave amplitude) is proportional to the COF and sliding velocity. In other words, the displacements during the vibrations in the  $x$ - and  $y$ -directions have the form

$$u(x, y, t) = U_0(x, y)e^{(\pm\lambda i + \mu VC)t} \quad (6)$$

$$w(x, y, t) = W_0(x, y)e^{(\pm\lambda i + \mu VC)t} \quad (7)$$

where  $U_0$  and  $W_0$  are the modes,  $\lambda$  is the frequency, and  $C$  is a constant. The real part of the term under the exponent  $\mu VC$  is the rate of growth of the instability (Fig. 2b).

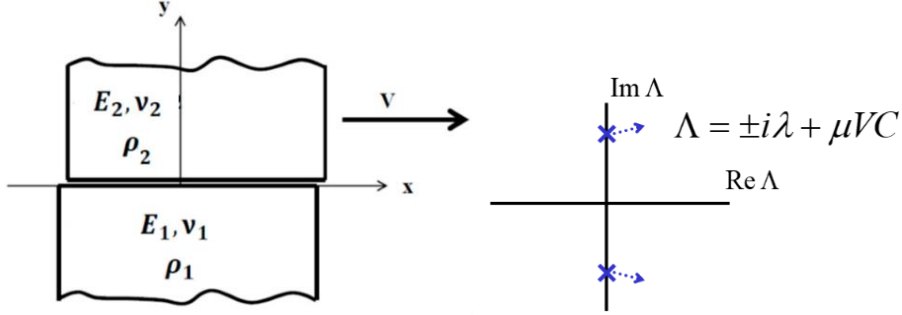


**Fig. 2** (a) Two elastic half-spaces sliding relative to one another. (b) Position of complex eigenvalues characterizing instabilities of dynamic solutions

Renardy [27] established ill-posedness of the frictional sliding of an elastic surface in contact with a rigid surface. Ranjith and Rice [28] showed that the dynamic sliding of dissimilar half-spaces is ill-posed in the sense that in the limit of short wavelength of the interfacial waves the degree of instability is inversely proportional to the wavelength and unbounded. In other words, for the wavenumber  $k$ ,

$$U_0(x, y) = u_0(y) \cos\left(\frac{kx}{2\pi}\right) \quad (8)$$

$$W_0(x, y) = w_0(y) \cos\left(\frac{kx}{2\pi}\right) \quad (9)$$

the degree of instability is proportional to the wavenumber,  $C \sim k$ , in the short wavelength limit  $1/k \rightarrow 0$ .

Ranjith and Rice also suggested a way of regularizing the ill-posedness by modifying the friction law and introducing the so-called rate-and-state friction with internal variables [28]. Generally speaking, dynamic instabilities and ill-posedness in the short wavelength limit are closely related to one another.

### 2.3 Instabilities of Velocity-Dependent Friction

Another type of friction-induced instability is due to frictional weakening. As the force of friction decreases with the increasing velocity, a small fluctuation of sliding velocity can trigger a positive feedback loop. A higher velocity leads to lower friction, lower resistance, acceleration, and further uncontrolled increasing velocity. On the other hand, a lower velocity leads to higher frictional resistance, consequent deceleration and further decreasing velocity. The sliding velocity cannot grow forever, and the growth continues until the frictional weakening stops. In that case the sliding velocity can drop due to increased friction. This leads to friction-induced self-excited non-linear vibrations, such as the stick-slip [17, 29].

It has been suggested in the literature on friction-induced self-organization, that a thermodynamic stability criterion can be applied to the frictional sliding [29-31]. In particular, the entropy production rate,  $\dot{S}$ , controls the stability of a tribological system at a steady state. The entropy production rate for such a system is often at a minimum. The stability is governed by the sign of the second variation of the entropy production rate

$\dot{S} = \mu WV/T$ , where  $W$  is the normal load,  $\mu W$  is the friction force,  $V$  is the sliding velocity and  $T$  is temperature [17-19]. The second variation is then given by

$$\delta^2 \dot{S} = \frac{W}{T} \delta W \delta \mu = \frac{W}{T} \frac{d\mu}{dV} (\delta V)^2 > 0 \quad (10)$$

and the stability is dependent on the sign of  $\frac{d\mu}{dV}$ .

In a more complex case, the COF may depend on a structural parameter of the material,  $\varphi$  (e.g., the thickness of a film at the surface of the material, Fig. 3). The stability criterion can then be written as

$$\delta^2 \dot{S} = \frac{WV}{T} \frac{d^2 \mu}{d\varphi^2} (\delta \varphi)^2 \quad (11)$$

If the stability condition is violated for a certain value of  $\varphi$ , then further growth of the film will result in decreasing friction and wear, which will facilitate the further growth of the film [17, 29]. Such an *in situ* formed tribofilm can often play a protective role as it minimizes friction and wear. The standard example is a Cu film formed at the Bronze-Steel frictional interface due to migration of  $\text{Cu}^+$  ions from the bulk of bronze to the interfaces caused by the temperature gradient near the interface.

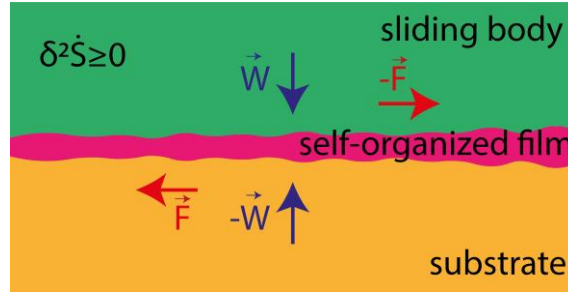


**Fig. 3** Schematic showing *in situ* formed tribofilm at a bi-material unstable interface

Similarly, the parameter  $\varphi$  can mean the surface roughness or the rate of wear. Eq. (10) provides a very general criterion of frictional stability [17, 29].

#### 2.4 Instabilities of the Onset of Sliding

The onset of frictional sliding is another process which has many features of destabilization. It has been suggested that the initiation of sliding has many features similar to fracture along the interface, in particular, to the shear (mode-II) crack initiation (Fig. 4) due to rapid dynamic effects [17, 20] during the transition from static to kinetic friction. Stress distribution during the onset of sliding is consistent with crack propagation model based on the linear elastic fracture mechanics [32], while frictional dynamic instabilities at a bimaterial interface are of the same type as the Adams instabilities [33].

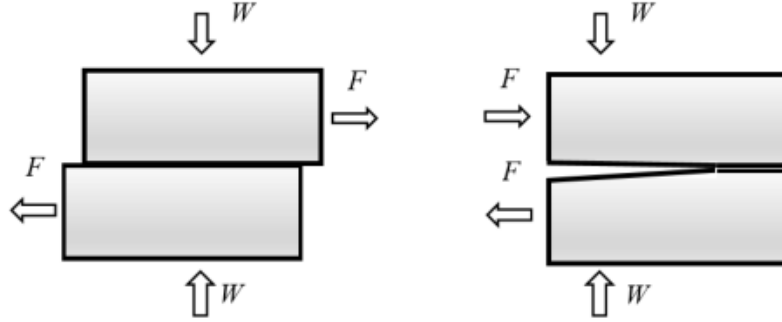


**Fig. 4** The similarity of mechanical systems with sliding friction (left) and mode II (shear) crack (right)

### 3. MACHINE-LEARNING METHODS

Since dynamically unstable motion often cannot be simulated by traditional computational methods due to the divergence, novel statistical ML methods can be applied. The difference between traditional and ML methods is that the dependency between the input and output parameters in the latter is expressed in the form of an algorithm, instead of a formula or equation, which usually governs traditional systems.

#### 3.1 Topological Data Analysis

The method of Topological Data Analysis (TDA) including the persistence analysis shows how these topological features, such as holes and voids, depend on the spatial resolution [34]. The idea of this method is that experimental data points are presented as points in an abstract multi-dimensional data space. Following that, the above-mentioned topological features are sought.

An example of the input may be a visual image (a photograph) presented as a matrix of  $256 \times 256$  pixels or a map representing a surface roughness surface  $z_{ij}(x_i, y_j)$  with  $1 \leq i, j \leq 256$ . Such matrix can be divided into  $3 \times 3$  square pixel patches, with each patch forming a data point in a 9D space thus providing a large number of  $254 \times 254 = 64516$  patches / data points per image. These data points have a certain distribution in the 9D data space, which depends on various features of the image or a random rough surface. Thus, due to the anisotropy of the images (e.g., horizontal and vertical features dominating over those inclined under an arbitrary angle) the points would form certain structures that can be detected by the TDA algorithms.

For surface roughness data, TDA provides “persistence diagrams” and “barcodes” which represent the dependency of topological invariants on the length scale resolution. Topological invariants are connected components ( $H_0$ ), 1D holes ( $H_1$ ), and higher dimensional voids ( $H_2, H_3$ , etc.). The intervals of the feature appearance and disappearance are plotted as bars in the barcode diagram or as a point characterizing their appearance and disappearance in the persistence diagram (see Ref. [34] for more technical details). These features show the types of anisotropic features at a certain scale level. Thus, the output of the algorithm is a dependency of anisotropic features on scale.

### 3.2 The Onset of Sliding

One area where TAD can be used is the analysis of the onset of sliding. The frictional sliding of two elastic rough surfaces may involve three local states: stick, slip, and separation. The growth of local slip zones and their merger in a one single-connected slip zone during the increase of shear loading facilitates the onset of global sliding. Here we suggest a simplified procedure of studying this transition to a single-connected slip zone by a similar transition of stick-separation to a single-connected stick zone during the increase of normal loading.

When a rough random elastic surface  $z(x,y)$  is pressed against a flat surface by the normal load force  $W$ , the asperities of a rough surface deform. The exact determination of the stress distribution would require a solution of the contact elasticity problem. However, it is appropriate to assume that stresses at asperity contacts are roughly proportional to the height of the asperity,  $\sigma(x,y) \sim z(x,y)$ . With increasing load  $W$ , stresses grow, however the static friction inequality can hold,  $\tau(x,y) < \mu\sigma(x,y)$ . The transition to the slip state is given locally by the relationship  $\tau(x,y) = \mu\sigma(x,y)$ . The stress state at every point of contact depends both on the shear load at that point and, due to the elastic relaxation, on the states of neighboring points thus forming slip zones of correlated neighboring points. The “islands” of the slip zones grow with the shear load until they merge forming a network of slip zones (Fig. 5). This makes the transition to the global sliding of the two bodies in contact similar to classical problems of percolation. In such problems, the slip zone diameters are usually related to the distance from the critical load,  $W_{cr}$ , by a power law  $d \sim (W - W_{cr})^\gamma$ , where  $\gamma$  is the critical exponent [17].

While it is difficult to evaluate the map of the slip zones at a frictional interface, one can obtain an experimental height profile of a surface,  $z(x,y)$ . Given  $\sigma(x,y) \sim z(x,y)$ , one can argue that the condition of the local transition to slip,  $\tau(x,y) = \mu\sigma(x,y)$ , could be replaced by a similar condition  $\tau_f = Kz(x,y)$ , where  $\tau_f$  is the frictional strength of the interface, and  $K$  is a coefficient. Therefore, the study of the transition can be replaced by the study of the separation zones. Fig. 5 shows the cross-sections of rough bronze surface  $5 \times 5 \mu\text{m}$  sample measured by an Atomic Force Microscope (AFM) corresponding to layers at different heights from 1% (when 0% corresponds to the highest asperity) to 87% (when 100% corresponds to deepest valley). The surface shown in dark color changes from separated islands to a single-connected area between 37% and 47%. It is anticipated that at the transition point critical phenomena can occur, which are typical to the phase transition. These phenomena would also correspond to the onset of sliding, which is a rapid dynamic event that is difficult to study by traditional methods.

In this case, the rough surface serves as an input of the algorithm, while quantitative characteristics of the transition (e.g., critical exponents relating the dependency of the slip zone diameters on the distance from the transition point) could be the output.

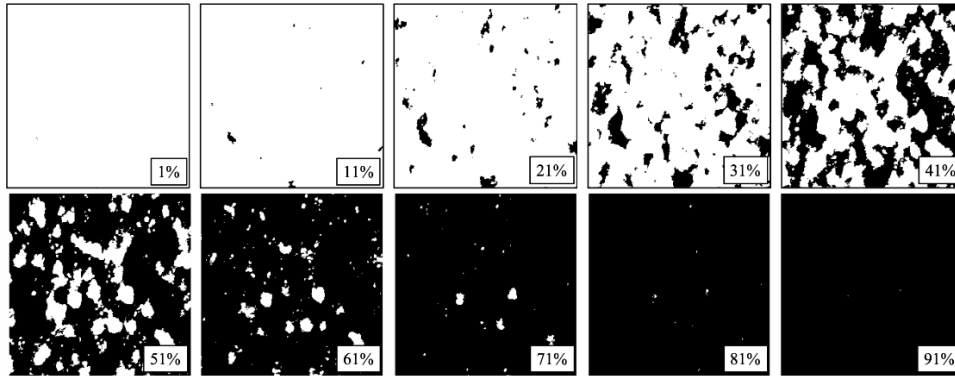


**Fig. 5** The transition from separation to contact with increasing normal load at the interface between a rough deformable and flat rigid surface

#### 4. CONCLUSIONS

Many modern problems of contact mechanics and tribology involve unstable motion or unstable solutions, which make it difficult to solve them by traditional approaches. Dry friction can cause dynamic instabilities, which are often related to the ill-posedness of mechanical models of the Coulombian friction with unlimited rate of instability in the short-wavelength limit of the solution. Various ways of regularization of the ill-posedness have been suggested in the literature. Unstable motion is effectively unpredictable from the initial conditions, since any small fluctuation grows exponentially with time.

We have suggested a threefold classification of dynamic possible solutions: (i) static problems, (ii) dynamic problems with stable solutions, and (iii) dynamic problems with unstable solutions. For unstable or close to instability solutions, new methods of analysis are suggested.

One way to handle the unstable motion is to apply statistical and Machine Learning tools. For such methods, structure-property dependencies are often expressed in the form of an algorithm, rather than as an equation.

The TDA method can provide scale dependency of characteristic features of a random rough surface, such as directions of anisotropy, if present.

The onset of sliding can be studied with the TDA tools and with methods of phase transition analysis, such as critical exponents.

In general, the unstable nature of many frictional processes leads to the novel mathematical and computational methods of tribological data analysis.

**Acknowledgement:** *This work was presented at the International Workshop “Interplay of Mechanics, Tribology, and Materials Science” at Samarkand State University (Uzbekistan), 4-6 September, 2023. Support from the Priority-2030 program (ITMO University) is acknowledged. The authors would like to thank Prof. Valentin Popov (TU Berlin) and Ekaterina V. Skorb (ITMO University). M. N. acknowledges sabbatical support from UWM.*

## REFERENCES

1. Popov, V.L., 2018, *Is Tribology Approaching its Golden Age? Grand Challenges in Engineering Education and Tribological Research*, *Frontiers in Mechanical Engineering*, 4, 16.
2. Ostermeyer, G.-P., Müller, M., 2006, *Dynamic interaction of friction and surface topography in brake systems*, *Tribology International*, 39(5), pp. 370-380.
3. Popov, V.L., Poliakov, A.M. Pakhaliuk, V.I., 2023, *In silico evaluation of the mechanical stimulation effect on the regenerative rehabilitation for the articular cartilage local defects*, *Frontiers in Medicine*, 10, 1134786.
4. Filippov, A.E., Popov, V.L., 2010, *Modified Burridge–Knopoff model with state dependent friction*, *Tribology International*, 43(8), pp. 1392-1399.
5. Lyashenko, I.A., Popov, V.L., Borysiuk, V., 2023, *Indentation and Detachment in Adhesive Contacts between Soft Elastomer and Rigid Indenter at Simultaneous Motion in Normal and Tangential Direction: Experiments and Simulations*, *Biomimetics*, 8(6), 477.
6. Popov, V.L., Heß, M., Willert, E., 2019, *Handbook of Contact Mechanics. Exact Solutions of Axisymmetric Contact Problems*, Springer, Berlin, Heidelberg, 363 p.
7. Popov, V.L., 2021, *Energetic criterion for adhesion in viscoelastic contacts with non-entropic surface interaction*, *Reports in Mechanical Engineering*, 2(1), pp. 57-64.
8. Forsbach, F., Heß, M., Papangelo, A., 2023, *A two-scale FEM-BAM approach for fingerpad friction under electroadhesion*, *Frontiers in Mechanical Engineering*, 8, 1074393.
9. Lyashenko, I.A., Pham, T.H., Popov, V.L., 2024, *Effect of Indentation Depth on Friction Coefficient in Adhesive Contacts: Experiment and Simulation*, *Biomimetics*, 9(1), 52.
10. Li, Q., Lyashenko, I.A., Pohrt, R., Popov, V.L., 2022, *Influence of a Soft Elastic Layer on Adhesion of Rough Surfaces*, in: Borodich, F.M., Jun, X. (Eds.), *Contact Problems for Soft, Biological and Bioinspired Materials. Biologically-Inspired Systems*, vol. 15, pp. 93-102.
11. Argatov, I., 2019, *Artificial neural networks (ANNs) as a novel modeling technique in tribology*, *Frontiers in Mechanical Engineering*, 5, 30.
12. Bhattacharya, S., Chakraborty, S., 2023, *Prediction of Responses in a CNC Milling Operation Using Random Forest Regressor*, *Facta Universitatis-Series Mechanical Engineering*, 21(4) pp. 685-700.
13. Michel, A. N., Hou, L., Liu, D., 2008, *Stability of dynamical systems*, Birkhäuser, Boston, 653 p.
14. Galanti, B., Tsinober, A., 2004, *Is turbulence ergodic?*, *Physical Letters A*, 330(3-4), pp. 173-180.
15. Korolev, I., Aliev, T., Orlova, T., Ulasevich, S.A., Nosonovsky, M., Skorb, E.V., 2022, *When Bubbles Are Not Spherical: Artificial Intelligence Analysis of Ultrasonic Cavitation Bubbles in Solutions of Varying Concentrations*, *The Journal of Physical Chemistry B*, 26(16), pp. 3161-3169.
16. Hasan, M.S., Nosonovsky, M., 2022, *Triboinformatics: machine learning algorithms and data topology methods for tribology*, *Surface Innovations* 10(4-5), pp. 229-242.
17. Nosonovsky, M., Mortazavi, V., 2014, *Friction-Induced Vibrations and Self-Organization*, CRC Press: Boca Raton.
18. Popova, E., Popov, V.L., *The research works of Coulomb and Amontons and generalized laws of friction*, *Friction*, 3(2), pp. 183-190.
19. Miguel, M.-C, Moretti, P., Zaiser, M., Zapperi, S., 2005, *Statistical dynamics of dislocations in simple models of plastic deformation: Phase transitions and related phenomena*, *Materials Science and Engineering: A*, 400-401, pp. 191-198.
20. Nosonovsky, M., Breki, A., 2019, *Ternary Logic of Motion to Resolve Kinematic Frictional Paradoxes*, *Entropy*, 21, 620.
21. Anh, L.X., 1990, *The Painlevé paradoxes and the law of motion of mechanical systems with coulomb friction*, *Journal of Applied Mathematics and Mechanics*, 54, pp. 430-438.
22. Anh, L.X., 2003, *Dynamics of Mechanical Systems with Coulomb Friction*, Springer: New York, NY, USA.
23. Génot, F., Brogliato, B., 1999, *New results on Painlevé paradoxes*, *Eur. J. Mech. A*, 18(4), pp. 653-678.
24. Champneys, A.R., Varkonyi, P.L., 2016, *The Painlevé paradox in contact mechanics*, *IMA Journal of Applied Mathematics*, 81(3), pp. 538-588.
25. Adams, G. G., 1995, *Self-excited oscillations of two elastic half-spaces sliding with a constant coefficient of friction*, *Journal of Applied Mechanics*, 62, pp. 867-872.
26. Nosonovsky, M. Adams, G.G., 2004, *Vibration and stability of frictional sliding of two elastic bodies with a wavy contact interface*, *Journal of Applied Mechanics*, 71, pp. 154-161.
27. Renardy, M., 1992, *Ill-posedness at the boundary for elastic solids sliding under Coulomb friction*, *Journal of Elasticity*, 27, pp. 281-287.
28. Ranjith, K., Rice, J.R., 2001, *Slip dynamics at an interface between dissimilar materials*, *Journal of Mechanics and Physics of Solids*, 49, pp. 341-361.
29. Nosonovsky, M., 2010, *Entropy in Tribology: in the Search for Applications*, *Entropy*, 12, pp. 1345-1390.

30. Gershman, I.S., 2006, *Formation of Secondary Structures and Self-Organization Process of Tribosystems during Friction with the Collection of Electric Current*, in: Fox-Rabinovich, G.S., Totten, G.E., (Eds.), *Self-Organization during Friction. Advanced Surface-Engineered Materials and Systems Design*, CRC Taylor & Francis: Boca Raton, FL, USA, 2006, pp. 197-230.
31. Fox-Rabinovich, G.S., Veldhuis, S.C., Kovalev, A.I., Wainstein, D. L., Gershman, I. S., Korshunov, S., Shuster, L.S., Endrino, J.L., 2007, *Features of self-organization in ion modified nanocrystalline plasma vapor deposited AlTiN coatings under severe tribological conditions*, *Journal of Applied Physics*, 102, 074305.
32. Svetlizky, I., Fineberg, J., 2014, *Classical shear cracks drive the onset of dry frictional motion*, *Nature*, 509, pp. 205-208.
33. Shlomain, H., Fineberg, J., 2016, *The structure of slip-pulses and supershear ruptures driving slip in bimaterial friction*, *Nature Communications*, 7, 11787.
34. Zhukov, M., Hasan M.S., Nesterov, P., Sabbouh, M., Burdulenko, O., Skorb, E.V., Nosonovsky, M., 2021, *Topological Data Analysis of Nanoscale Roughness in Brass Samples*, *ACS Applied Materials & Interfaces*, 14(1), pp. 2351-2359.